

# Nanomolecular HLA-DR10 Antibody Mimics: A Potent System for Molecular Targeted Therapy and Imaging

Gerald L. DeNardo,<sup>1</sup> Arutselvan Natarajan,<sup>1</sup> Saphon Hok,<sup>2</sup> Gary Mirick,<sup>1</sup> Sally J. DeNardo,<sup>1</sup>  
Michele Corzett,<sup>2</sup> Vladimir Sysko,<sup>1</sup> Joerg Lehmann,<sup>1</sup> Laurel Beckett,<sup>3</sup> and Rod Balhorn<sup>2</sup>

<sup>1</sup>University of California, Davis Medical Center, Sacramento, CA

<sup>2</sup>Lawrence Livermore National Laboratories, Livermore, CA

<sup>3</sup>University of California, Davis, Public Health Sciences, Davis, CA

## ABSTRACT

To mimic the molecular specificity and cell selectivity of monoclonal antibody (mAb) binding while decreasing size, nanomolecules (selective high-affinity ligands; SHALs), based on *in silico* modeling, have been created to bind to human leukocyte antigen-DR (HLA-DR10), a signaling receptor protein upregulated on the malignant B-lymphocytes of non-Hodgkin's lymphoma and chronic lymphocytic leukemia. SHALs were synthesized with a biotin or DOTA chelate (1,4,7,10-tetraazacyclododecane-*N,N',N'',N'''*-tetraacetic acid), using a solid-phase lysine-polyethyleneglycol backbone to link sets of ligands shown previously to bind to HLA-DR10. Using cell-binding and death assays and confocal microscopy, SHAL uptake, residualization, and cytotoxic activity were evaluated in HLA-DR10 expressing and nonexpressing live, human lymphoma cell lines. All of the SHALs tested were selective for, and accumulated in, expressing cells. Reflecting binding to HLA-DR10 inside the cells, SHALs having the Ct ligand (3-(2-([3-chloro-5-trifluoromethyl]-2-pyridinyl)oxy)-anilino)-3-oxopropanionic acid) residualized in expressing cells greater than 179 times more than accountable by cell-surface membrane HLA-DR10. Confocal microscopy confirmed the intracellular residualization of these SHALs. Importantly, SHALs with a Ct ligand had direct cytotoxic activity, similar in potency to that of Lym-1 mAb and rituximab, selectively for HLA-DR10 expressing lymphoma cells and xenografts. The results show that SHALs containing the Ct ligand residualize intracellularly and have cytotoxic effects mediated by HLA-DR10. These SHALs have extraordinary potential as novel molecules for the selective targeting of lymphoma and leukemia for molecular therapy and imaging. Further, these SHALs can be used to transport and residualize cytotoxic agents near critical sites inside these malignant cells.

**Key words:** antibodies, nanomolecules, ligands, HLA-DR, lymphoma, therapy, imaging

## INTRODUCTION

*"Nothing is too wonderful to be true if it be consistent with the laws of nature."*

—Michael Faraday

Address reprint requests to: Gerald L. DeNardo; University of California, Davis Medical Center; 1508 Alhambra Boulevard, Room 3100, Sacramento, CA 95816; Tel.: (916) 734-3787; Fax: (916) 703-5014  
E-mail: gldenardo@ucdavis.edu

Most chemotherapeutic drugs penetrate and, as readily, exit cells and tissues. Because cell uptake is not selective, the effectiveness of these drugs is limited by their toxicity. Other drugs of small size (e.g., fluorine-18 [<sup>18</sup>F] deoxyglucose and iodine-131 [<sup>131</sup>I] sodium iodide), are routinely used for imaging because they also bind to the cancer cells. Because <sup>131</sup>I rapidly accumulates in thyroid cancer (in the absence of normal thyroid tissue), this drug has a major role in the management of metastatic thyroid cancer and is a

paradigm for molecular-targeted systemic radiotherapy.

Larger molecules, such as monoclonal antibodies (mAbs), have also been used for these purposes. Rituximab (Rituxan<sup>®</sup>; Biogen Idec Inc., Cambridge, MA, and Genentech Inc., South San Francisco, CA), a chimeric anti-CD20 mAb, induces cells, to which it binds, to die. To increase these effects and to permit imaging, radionuclides have been conjugated to anti-CD20 mAbs. Ibritumomab (Zevalin<sup>®</sup>; Biogen Idec Inc.), the mouse parent of rituximab, labeled with yttrium-90 (<sup>90</sup>Y), induced higher response rates than rituximab in a randomized trial in patients with non-Hodgkin's lymphoma (NHL).<sup>1</sup> Similarly, the anti-CD20 mAb, tositumomab (Bexxar<sup>®</sup>; GlaxoSmithKline, Research Triangle Park, NC), labeled with <sup>131</sup>I, induced more favorable therapeutic outcomes than chemotherapy.<sup>2</sup> Another mAb, Lym-1, has also been shown to be an effective carrier of radionuclides for systemic radiotherapy in patients<sup>3</sup> and to have antilymphoma activity greater than that of rituximab after ligation of HLA-DR because of cell-death signaling.<sup>4-6</sup>

Using *in silico* modeling, novel nanomolecules were designed to serve as carriers of cell toxins, such as radionuclides, by mimicking the specific binding of Lym-1 mAb to the  $\beta$ -subunit of human leukocyte antigen-DR (HLA-DR) in the region of residues shown critical for Lym-1 binding and cytotoxicity in lymphoma cell lines of B-cell genotypes.<sup>7,8</sup> Binding of these selective high-affinity ligands (SHALs) mimics that of mAbs because multiple contacts between residues on the surface of the SHAL and its target protein provide high specificity and affinity.<sup>9,10</sup> Contrarywise, SHALs mimic the pharmacokinetic behavior of sodium iodide, because they are small and rapidly trapped by HLA-DR10-expressing lymphoma tissue or excreted in the urine.

Although all of the SHALs have discriminated HLA-DR10 expressing from nonexpressing malignant cells, mimicking Lym-1,<sup>11-13</sup> and exhibited small-molecule pharmacokinetic behavior,<sup>11,14</sup> earlier SHALs tested showed no antilymphoma activity.<sup>12</sup> To increase binding and selectivity and, therefore, SHAL residence time in NHL tissue, SHALs having a Ct ligand (3-(2-((3-chloro-5-trifluoromethyl)-2-pyridinyl)oxy)-anilino)-3-oxopropanionic acid) for a third docking site on HLA-DR10 were synthesized.<sup>14,15</sup>

In this paper, we characterize the cellular fates and effects of both a tridentate and a dimeric, tri-

dentate SHAL, each containing the Ct ligand, compare their behavior with those of other bidentate SHALs containing and lacking the Ct ligand, and show that the Ct ligand SHALs residualize in HLA-DR10-expressing human lymphoma cells. Although intended to be cell-specific carriers for molecular therapy and imaging, SHALs containing the Ct ligand exhibited direct antilymphoma (i.e., cytotoxic) activity in the absence of a radionuclide. Because these SHALs readily pass through cell membranes, they also have enormous potential for selective intracellular delivery of a variety of cytotoxic agents.

## MATERIALS AND METHODS

### Reagents and Cell Lines

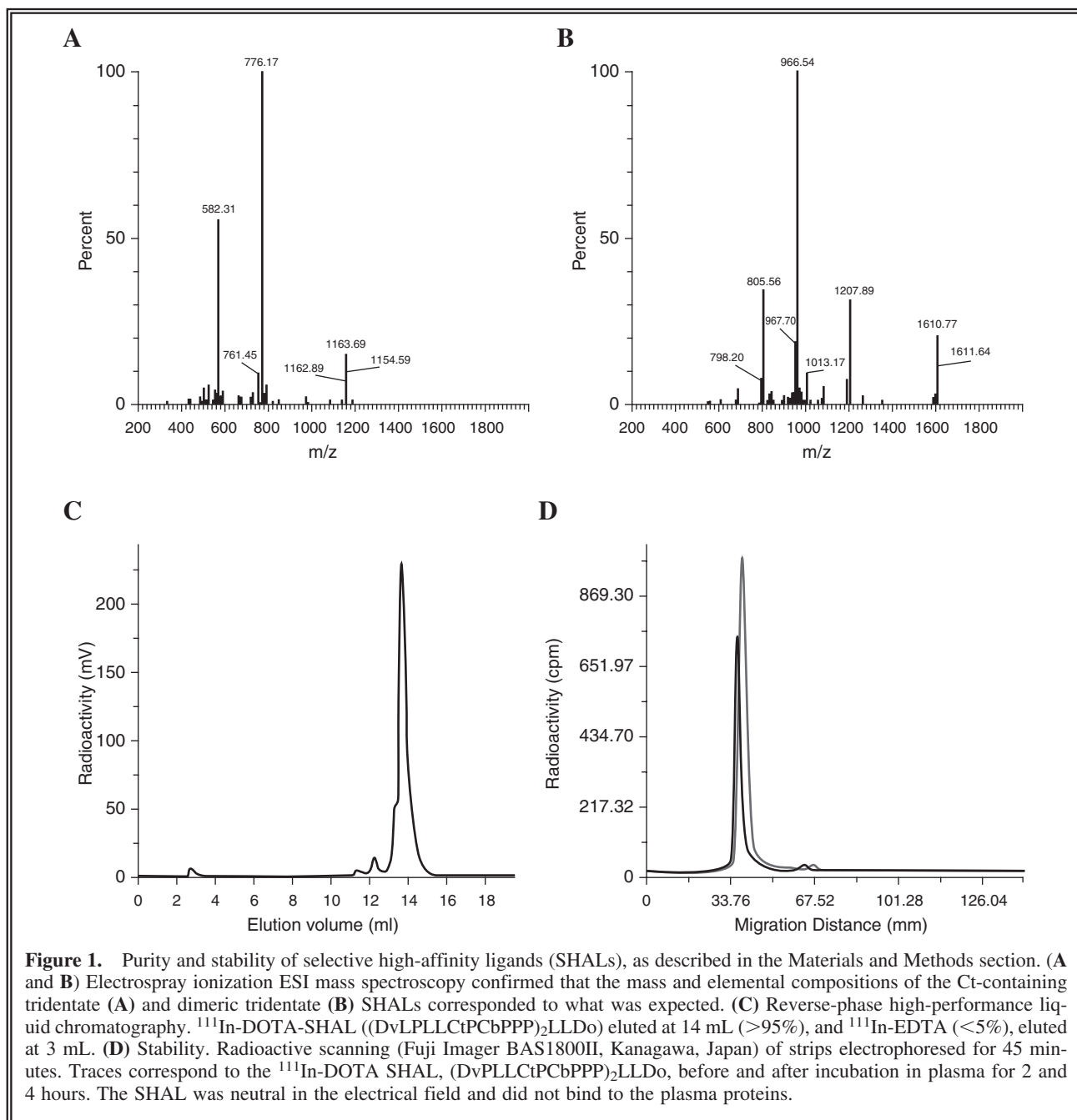
Murine Lym-1 (Peregrine Pharmaceuticals, Tustin, CA) was generated by using Raji malignant lymphocytes as the immunogen. Murine and chimeric (A. Epstein, Los Angeles, CA) Lym-1 bind to an epitope in the beta-subunit of HLA-DR10 and related HLA-DR proteins expressed on malignant B-cells.<sup>7,8,16</sup> HLA-DR10 protein that is expressed by antigen-presenting cells was isolated from Raji Burkitt's human lymphoma B-cells and purified on a Lym-1 affinity column, as described previously.<sup>13</sup> Two HLA-DR10-expressing human B-cell lymphoma lines, Raji (American Type Culture Collection, Manassas, VA) and SU-DHL4 (A. Epstein), and two non-expressing human T-cell lymphoma/leukemia lines, Jurkat's, and CEM (American Type Culture Collection), grown as recommended, were used for the experiments.

### Drug Design and Chemistry

Using homology modeling, residues critical for Lym-1 binding were mapped on a three-dimensional (3D) model of the HLA-DR10 beta-subunit.<sup>13</sup> Cavities within the Lym-1 epitope of the protein were identified by using SPHGEN.<sup>17,18</sup> After identifying ligands predicted to bind to the cavities by using computational docking, a combination of nuclear magnetic resonance (NMR) spectroscopy, surface plasmon resonance (Biacore 3000; Biacore, Piscataway, NJ), and competitive binding experiments were used to confirm that the ligands bound to different sites on HLA-DR10 protein. To create SHALs, ligands were conjugated to the ends of polyethylene glycol (PEG) monomers through the alpha and ep-

silon amines of the N-terminal lysine, using Fmoc solid-phase chemistry, as previously described.<sup>15</sup> The same process was used to synthesize the tridentate SHAL by linking together the three ligands, dabsylvaline (Dv), 4-[4-(4-chlorobenzyl)piperazino]-3-nitrobenzenecarboxylic acid (Cb), and Ct. The Dv ligand was attached to the  $\alpha$ -amine of the second lysine residue spaced with a PEG, and the Cb ligand was attached to the  $\alpha$ -amine of the third lysine, again spaced with a

PEG. Last, the Ct ligand was directly attached to the  $\epsilon$ -amine of the third lysine from the  $\epsilon$ -amine of the second lysine residue. For the dimeric, tridentate motif, one additional lysine residue, linked to the  $\alpha$ -amine of the first lysine, was used to construct two equivalent branching "SHALs" by inserting three consecutive PEG units at the alpha and epsilon amines. The  $\epsilon$ -amino group of the first lysine was used to attach a biotin or DOTA chelate (1,4,7,10-tetraazacyclododecane-



N,N',N'',N'''-tetraacetic acid). The reaction solution was purified by using reverse-phase high-performance liquid chromatography (RP-HPLC). Analytic electrospray ionization-mass spectrometry (Agilent 1100 instrument, Waters Symmetry C18 column, Agilent, Santa Clara, CA) confirmed the elemental and mass composition of each of the SHALs (Fig. 1). The SHALs studied herein and their corresponding acronyms are shown in Table 1, and the chemical structures in two dimensions and the acronyms for the Ct-containing tridentate and dimeric, tridentate SHALs are shown in Figure 2. Using surface plasmon resonance (BIAcore 3000), SHAL binding to isolated or recombinant HLA-DR10 protein was observed to be in the nanomolar range, as previously described.<sup>13,19</sup> SHALs no longer bound after the addition of Lym-1.

DOTA-SHALs were labeled with <sup>111</sup>InCl<sub>3</sub> in 0.05M HCl (MDS Nordion, Vancouver, Canada), as previously described.<sup>11,15</sup> Briefly, the reaction mixture was adjusted to pH 6–7 by adding 4 M NH<sub>4</sub>OAc, incubated for 1 hour at 37°C, then 0.1 M of ethylenediaminetetraacetic acid (EDTA) was added to sequester free <sup>111</sup>In<sup>3+</sup>. The reaction mixture was purified by using RP-HPLC. The purity of the products ranged from 90% to 95%.

The stability of each <sup>111</sup>In-DOTA-SHAL in plasma was assessed, as previously described, by using cellulose acetate electrophoresis for 45 minutes in tris-barbital-sodium buffer (pH 8.6).<sup>11,14</sup> Strips were imaged by using a phosphor imager (Fuji BAS1800II, Kanagawa, Japan), and SHAL electromobility was compared with those of the plasma proteins. Plasma aliquots were also

**Table 1.** Multidentate and Dimeric, Multidentate SHALs<sup>a</sup> Compared and Their Molecular Weight (MW) in Daltons

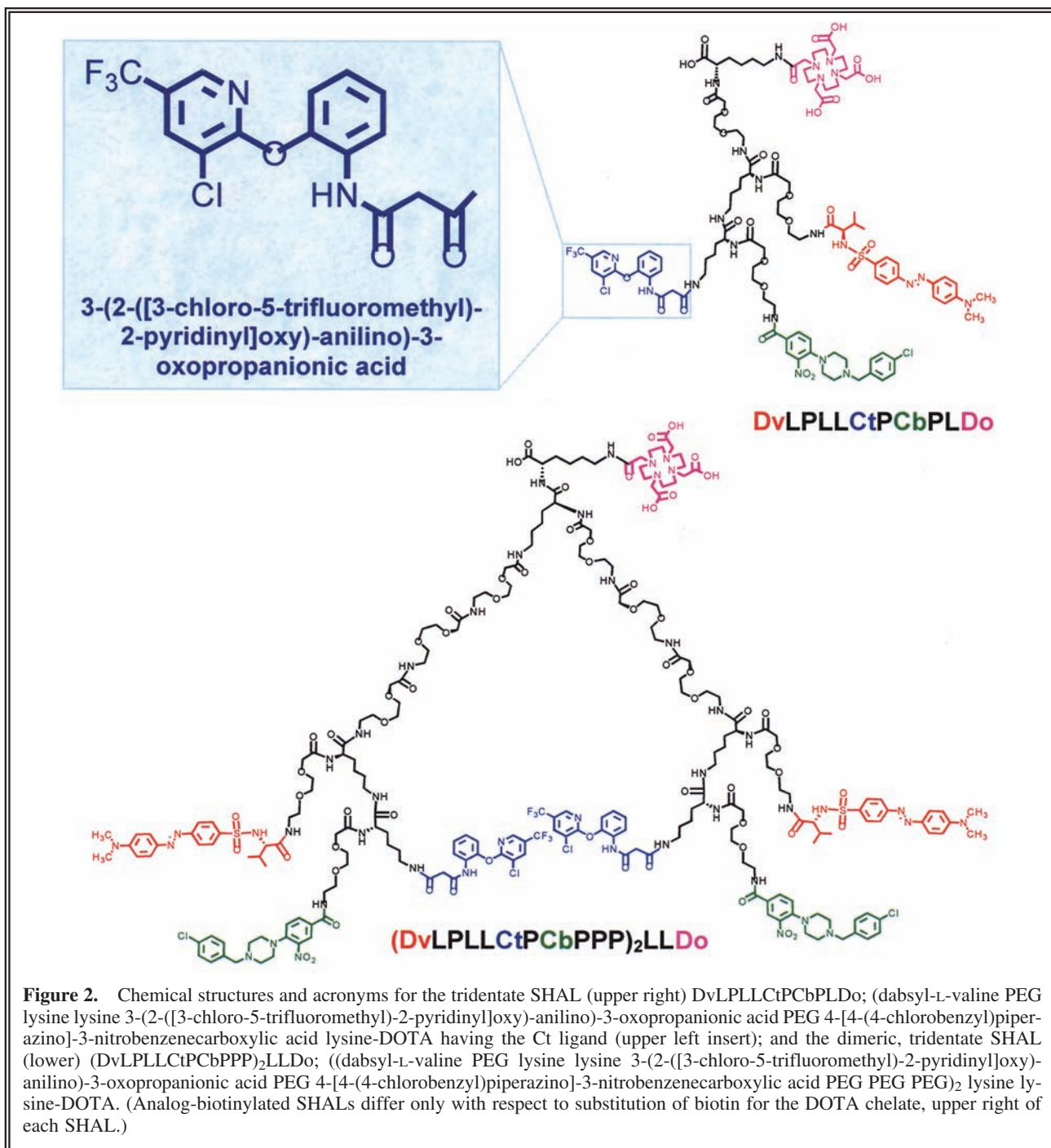
<i>Acronym</i>	<i>Identity</i>	<i>MW</i>
<b>Multidentate</b>		
LeacPLD	Acetylated 5-leu-enkephalin PEG lysine deoxycholate	1505
ItPLD	Triiodothyronine PEG lysine deoxycholate	1559
DvLPBaPL	Dabsyl-L-valine lysine PEG N-benzoyl-L-arginyl-4-amino-benzoic acid PEG lysine	1317
<b>CtLPTPL</b>	<b>3-(2-([3-chloro-5-trifluoromethyl]-2-pyridinyl]oxy)-anilino)-3-oxopropanionic acid lysine PEG L-thyronine PEG lysine<sup>a</sup></b>	<b>1163</b>
<b>CtLPBaPL</b>	<b>3-(2-([3-chloro-5-trifluoromethyl]-2-pyridinyl]oxy)-anilino)-3-oxopropanionic acid lysine PEG N-benzoyl-L-arginyl-4-amino-benzoic acid PEG lysine</b>	<b>1287</b>
<b>DvPLLCTPCbL</b>	<b>Dabsyl-L-valine PEG lysine lysine 3-(2-([3-chloro-5-trifluoromethyl]-2-pyridinyl]oxy)-anilino)-3-oxopropanionic acid PEG 4-[4-(4-chlorobenzyl)piperazino]-3-nitrobenzenecarboxylic acid lysine</b>	<b>1765</b>
<b>Dimeric, multidentate</b>		
(LeacPLD) <sub>2</sub> LP	(Acetylated 5-leu-enkephalin PEG lysine deoxycholate) <sub>2</sub> lysine PEG	3006
(ItPDP) <sub>2</sub> LL	(Triiodothyronine PEG deoxycholate PEG) <sub>2</sub> lysine lysine	3113
(DvLPBaP) <sub>2</sub> LL	(Dabsyl-L-valine lysine PEG N-benzoyl-L-arginyl-4-aminobenzoic acid PEG) <sub>2</sub> lysine lysine	2626
(DvLPBaPP) <sub>2</sub> LL	(Dabsyl-L-valine lysine PEG N-benzoyl-L-arginyl-4-aminobenzoic acid PEG PEG) <sub>2</sub> lysine lysine	2921
(DvLPBaPPP) <sub>2</sub> LL	(Dabsyl-L-valine lysine PEG N-benzoyl-L-arginyl-4-aminobenzoic acid PEG PEG PEG) <sub>2</sub> lysine lysine	3210
(DvLPBaPPPP) <sub>2</sub> LL	(Dabsyl-L-valine lysine PEG N-benzoyl-L-arginyl-4-aminobenzoic acid PEG PEG PEG PEG) <sub>2</sub> lysine lysine	3501
(DvLCsPBaPPP) <sub>2</sub> CsLL	(Dabsyl-L-valine lysine cysteic acid PEG N-benzoyl-L-arginyl-4-aminobenzoic acid PEG PEG PEG) <sub>2</sub> cysteic acid lysine lysine	3666
<b>(DvPLLCTPCbPPP)<sub>2</sub>LL</b>	<b>(Dabsyl-L-valine PEG lysine lysine 3-(2-([3-chloro-5-trifluoromethyl]-2-pyridinyl]oxy)-anilino)-3-oxopropanionic acid PEG 4-[4-(4-chlorobenzyl)piperazino]-3-nitrobenzenecarboxylic acid PEG PEG PEG)<sub>2</sub> lysine lysine</b>	<b>4267</b>

<sup>a</sup>SHALs containing the “Ct” ligand are in bold. DOTA on the SHAL contributes an additional 400 (or 244 for biotin) Daltons to the MW.

mixed with goat antihuman transferrin, antihuman albumin, antihuman IgG, or antihuman ceruloplasmin (Sigma, St. Louis, MO) in excess, then centrifuged at  $12,000\times g$  for 10 minutes. The activity of the supernatants and precipitates were measured by counting in a gamma-well counter (Pharmacia 1282 CompuGamma; Pharmacia, Inc., Piscataway, NJ). The  $^{111}\text{In}$ -DOTA-SHALs

did not bind to plasma proteins and were stable in plasma over 7 days (Fig. 1).

In summary, biotinylated and DOTA-SHALs were synthesized at high purity in multimilligram amounts. DOTA-SHALs were stably labeled with indium-111 ( $^{111}\text{In}$ ) at high efficiency, specific activity, and purity; median-specific activities were  $3.8 \text{ MBq}/\mu\text{g}$  ( $102 \mu\text{Ci}/\mu\text{g}$ ).



## Cell-Binding Assays

To assess SHAL binding to live cells, enzyme-linked immunosorbent assay (ELISA) assays were performed, as previously described.<sup>13</sup> Cells were incubated with biotinylated SHALs for 1 hour at RT or 4°C, washed, and transferred to a fresh plate. SA-HRP was added for 30 minutes, the cells pelleted, and 2,2'-azino-bis(3-ethylbenzothiazoline)-6-sulphonic acid substrate (ABTS) added for 20 minutes. HLA-DR-expressing cells bound more of the SHAL/SA-HRP complex, giving a greater signal.

The number of HLA-DR10 receptors on Raji cells was determined, as previously described.<sup>20</sup> Briefly, Lym-1, trace labeled with iodine-125 (<sup>125</sup>I), was added to varying amounts of unlabeled Lym-1 and incubated with  $1 \times 10^6$  cells in 5% bovine serum albumin and phosphate-buffered saline (BSA/PBS) for 1 hour at room temperature (RT). After separation by centrifugation, the cell pellet and supernatant were counted in a calibrated gamma well counter (Pharmacia 1282 CompuGamma, Piscataway, NJ). Scatchard analysis was used to estimate the number of receptors per cell.<sup>20</sup> The average for 10 assays was  $1.2 \pm 0.3 \times 10^6$  receptors per cell, or 2.3 pmoles per million cells.

## Live Cell Uptake and Residualization

To quantitate uptake and residualization of SHALs in live cells, an assay was performed by using serially diluted SHAL, as previously described.<sup>12</sup> Each SHAL labeled with <sup>111</sup>In, to which varying amounts of unlabeled SHAL had been added, was incubated with  $1 \times 10^6$  cells for 1 hour at RT. Cells were pelleted by centrifugation at 300g for 10 minutes. Cell pellet (bound) and supernatant were counted in a gamma-well counter. To determine the extent of SHAL residualization, an identical assay was performed, except that the cells were washed twice with PBS, washes pooled, and the cell pellet and pooled washes counted. Results represent the mean and standard deviation (SD) of replicate samples.

Immunohistochemistry was performed on formalin-fixed, paraffin-embedded NHL tissue sections from a patient after deparaffinization, as previously described.<sup>13</sup> Before incubation with Lym-1, antigen retrieval was accomplished by using high temperature. Slides were counterstained in Mayer's hematoxylin.

## Confocal Microscopy

Live cells were incubated with biotinylated chLym-1 or tridentate or dimeric, tridentate Ct-containing SHAL, then washed and fixed on slides before incubation with Streptavidin Alexa Fluor® (Invitrogen, Carlsbad, CA) 610 (red) to localize the SHAL or the chLym-1. The mounting medium contained DAPI, a nuclear stain. Laser scanning at 405 and 554 nm was performed by using an Olympus FV 100 confocal microscope (Center Valley, PA). Images were collected at focal planes 1  $\mu$  apart.

## Cytotoxicity Assay

Cells in log-growth phase were suspended in fresh media and counted after adding 10% trypan blue to distinguish nonviable from viable cells, as previously described.<sup>12</sup> In untreated samples, the cells multiplied and nonviable cells, initially less than 5% of total cells, remained at this level over the course of the assays. The assays were designed to detect antilymphoma activity from the Auger electrons of <sup>111</sup>In and to determine whether the observed effects could be blocked by

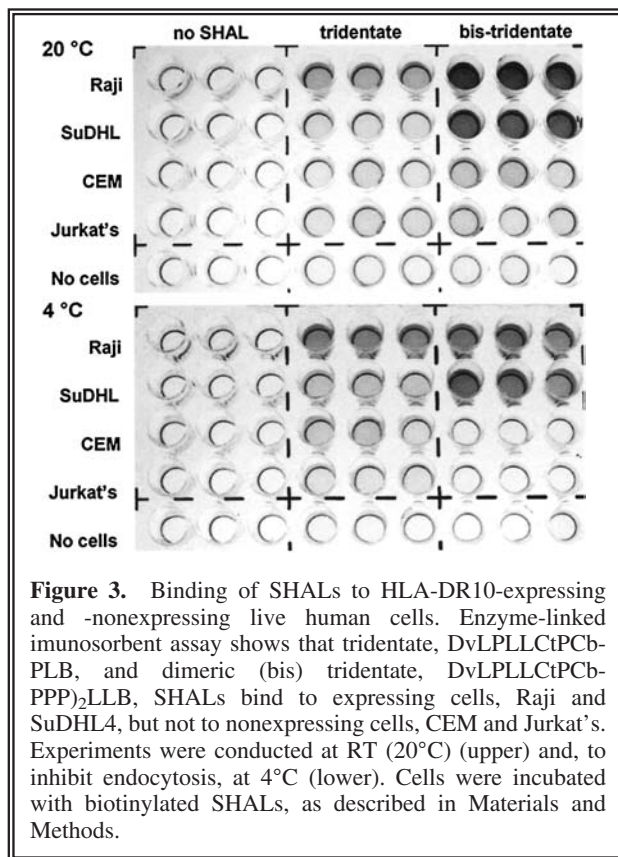


**Figure 3.** Binding of SHALs to HLA-DR10-expressing and -nonexpressing live human cells. Enzyme-linked immunosorbent assay shows that tridentate, DvLPLLCTPCb-PLB, and dimeric (bis) tridentate, DvLPLLCTPCb-PPP)<sub>2</sub>LLB, SHALs bind to expressing cells, Raji and SuDHL4, but not to nonexpressing cells, CEM and Jurkat's. Experiments were conducted at RT (20°C) (upper) and, to inhibit endocytosis, at 4°C (lower). Cells were incubated with biotinylated SHALs, as described in Materials and Methods.

treatment with 1000 ng of unlabeled SHAL. Tubes containing cells were incubated for 1 hour at RT with 100 ng of  $^{111}\text{In}$ -labeled SHAL, 100 ng of unlabeled SHAL as a control, or 100 ng of  $^{111}\text{In}$ -labeled SHAL after preincubation with 1000 ng of unlabeled SHAL. To remove unbound SHAL and  $^{111}\text{In}$  at the end of incubation, each tube was centrifuged at 300g for 10 minutes, the supernatant was removed, and then cells were washed twice in PBS (0.5 mL) for 15 minutes at RT. The cell pellet resuspended in fresh media and an aliquot of each pooled supernatant were counted to determine the amount of SHAL and  $^{111}\text{In}$  subsequently introduced into each of the triplicate wells. Cells from each tube were diluted to  $0.5 \times 10^6/\text{mL}$  in media with 10% fetal calf serum, aliquoted (200  $\mu\text{L}$ ) into sterile, flat-bottom wells and incubated at  $37^\circ\text{C}$ , 5%  $\text{CO}_2$ . Measurements of  $^{111}\text{In}$  activity indicated that the maximum amounts of  $^{111}\text{In}$  and SHAL were 39 nCi and 3 ng of tridentate SHAL, and 18 nCi and 1.4 ng of dimeric, tridentate SHAL for each well containing expressing cells, and less than 7 nCi and 0.5 ng of either SHAL for each well containing nonexpressing cells. After 1, 2, and 3 days, cells were resuspended and 90  $\mu\text{L}$  from each of the triplicate wells were added to 10  $\mu\text{L}$  of filtered trypan blue, and the refractile live and blue-stained dead cells were counted by using a microscope and hemocytometer.

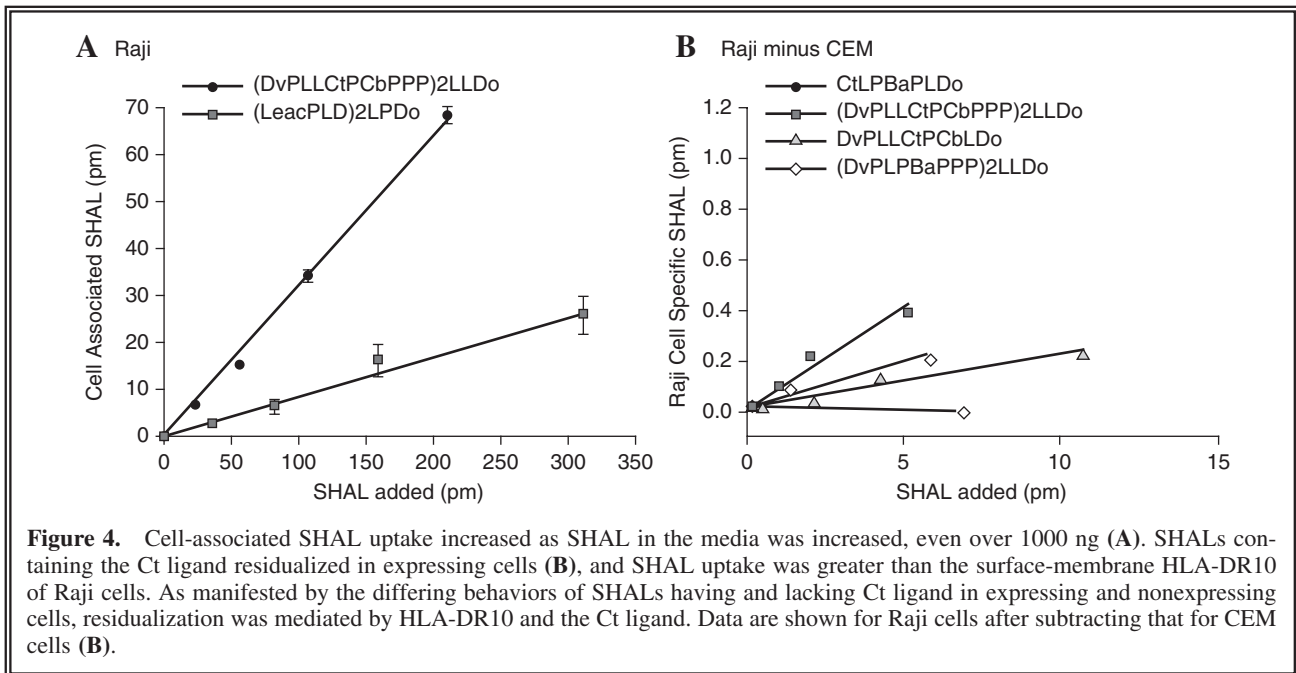
## Radiation-Absorbed Dose

The radiation-absorbed dose to the cells was estimated, using published methods and absorbed fractions.<sup>21</sup> Briefly, a measured mean cell diameter of 12  $\mu\text{m}$ , an estimated nuclear diameter of 10  $\mu\text{m}$ , and an S-value that assumed the  $^{111}\text{In}$  to be in the cytoplasm and the nucleus to be the radiation target were used. Calculations were based on the highest  $^{111}\text{In}$  activity measured for the wells. Radiation exposure received while the cells were incubating before washing was not included; it added less than 10% over 1 day and less than 5% over longer exposures. Because of their short range and the assay conditions, Auger electron exposure to neighboring cells was not considered. Despite these assumptions, the calculations represent an upper limit of exposure.<sup>22</sup>

## Biostatistical Analysis

The data are representative of replicate studies that showed reproducible results. For cell-uptake assays, the % binding was multiplied by the SHAL added to each well and reported as the mean  $\pm$  SD for each group of triplicates. When least mean squared linear regression was performed over the range of SHAL added, there was a good fit.

To assess the cytotoxic effect of the SHALs, a series of regression models, including a nonpara-



metric Wilcoxon test, were fitted to the fractional percentages and to the absolute numbers of nonviable cells as the outcomes, separately in HLA-DR10-expressing and -nonexpressing cells within an experiment. Predictors were included to estimate the effect of radiation dose, both as a linear dose response and—to check linearity—as indicators for the effects of additional  $^{111}\text{In}$  above the next lower levels, the effect of adding SHAL, the effect of dimeric, tridentate beyond tridentate SHAL, and the possible interaction of SHAL with radiation. Differences were deemed significant if  $p \leq 0.05$ .

## RESULTS

Although the SHALs differed with respect to the nature of the ligands and their number, and the

number of PEG monomers and lysines, all of the SHALs were electrically neutral and bound selectively to HLA-DR10 protein and expressing live cells.<sup>13,15</sup> In contrast to Lym-1, SHALs accumulated in the cells over an extended range because of internalization. Four SHALs, two bidentate, one tridentate, and one dimeric, tridentate, all containing the Ct ligand, exhibited even greater lymphoma cell uptake. To further assess the influence of the Ct ligand, additional studies were performed on the tridentate and the dimeric, tridentate SHAL in expressing and nonexpressing live lymphoma cells. These included studies of cell uptake and residualization (after washing) of both DOTA and biotinylated motifs at RT and at 4°C, confocal microscopy, and cytotoxicity assays, using unlabeled and  $^{111}\text{In}$ -labeled SHALs.

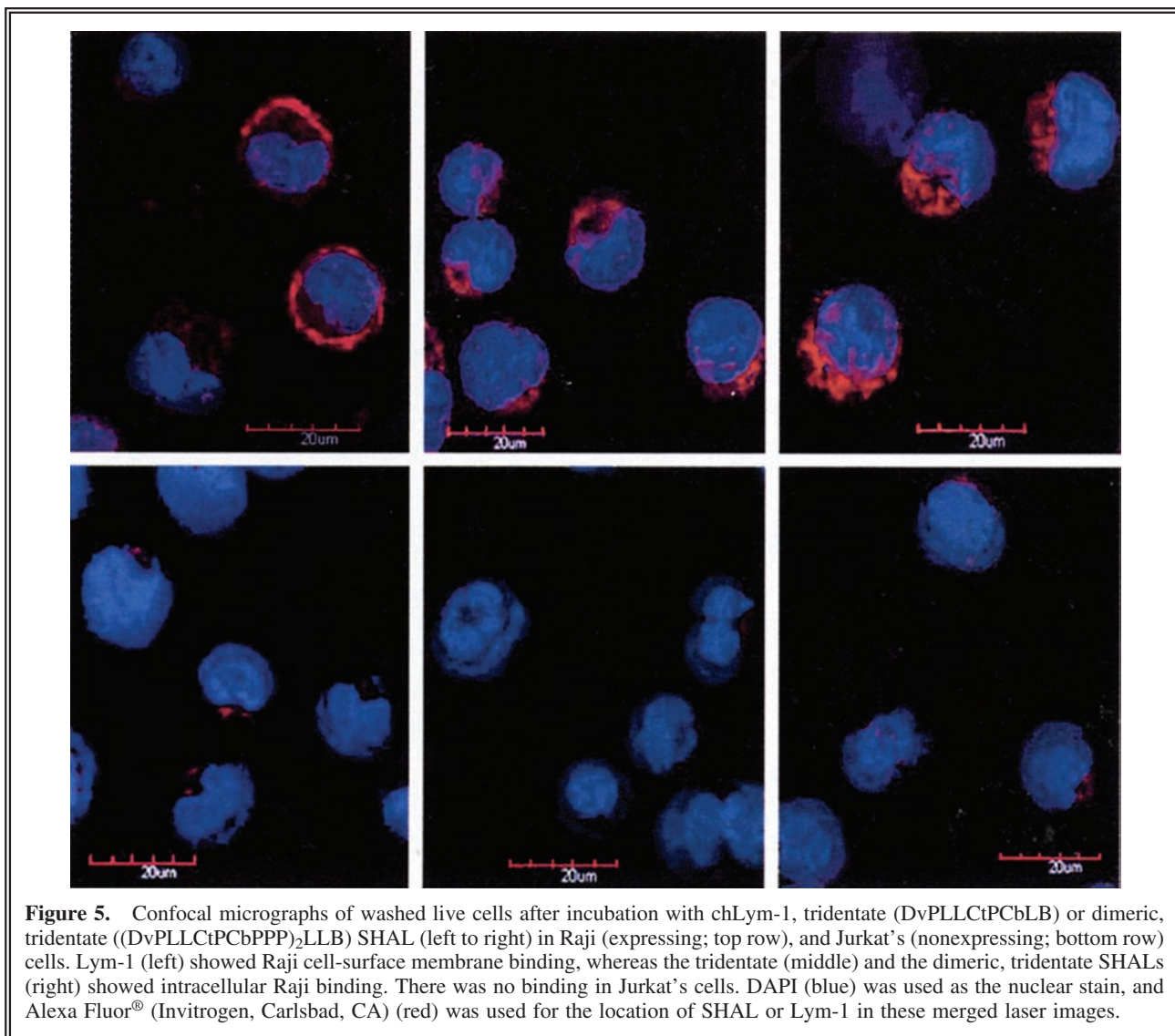


**Figure 5.** Confocal micrographs of washed live cells after incubation with chLym-1, tridentate (DvPLLCTPCbLB) or dimeric, tridentate ((DvPLLCTPCbPPP)<sub>2</sub>LLB) SHAL (left to right) in Raji (expressing; top row), and Jurkat's (nonexpressing; bottom row) cells. Lym-1 (left) showed Raji cell-surface membrane binding, whereas the tridentate (middle) and the dimeric, tridentate SHALs (right) showed intracellular Raji binding. There was no binding in Jurkat's cells. DAPI (blue) was used as the nuclear stain, and Alexa Fluor® (Invitrogen, Carlsbad, CA) (red) was used for the location of SHAL or Lym-1 in these merged laser images.

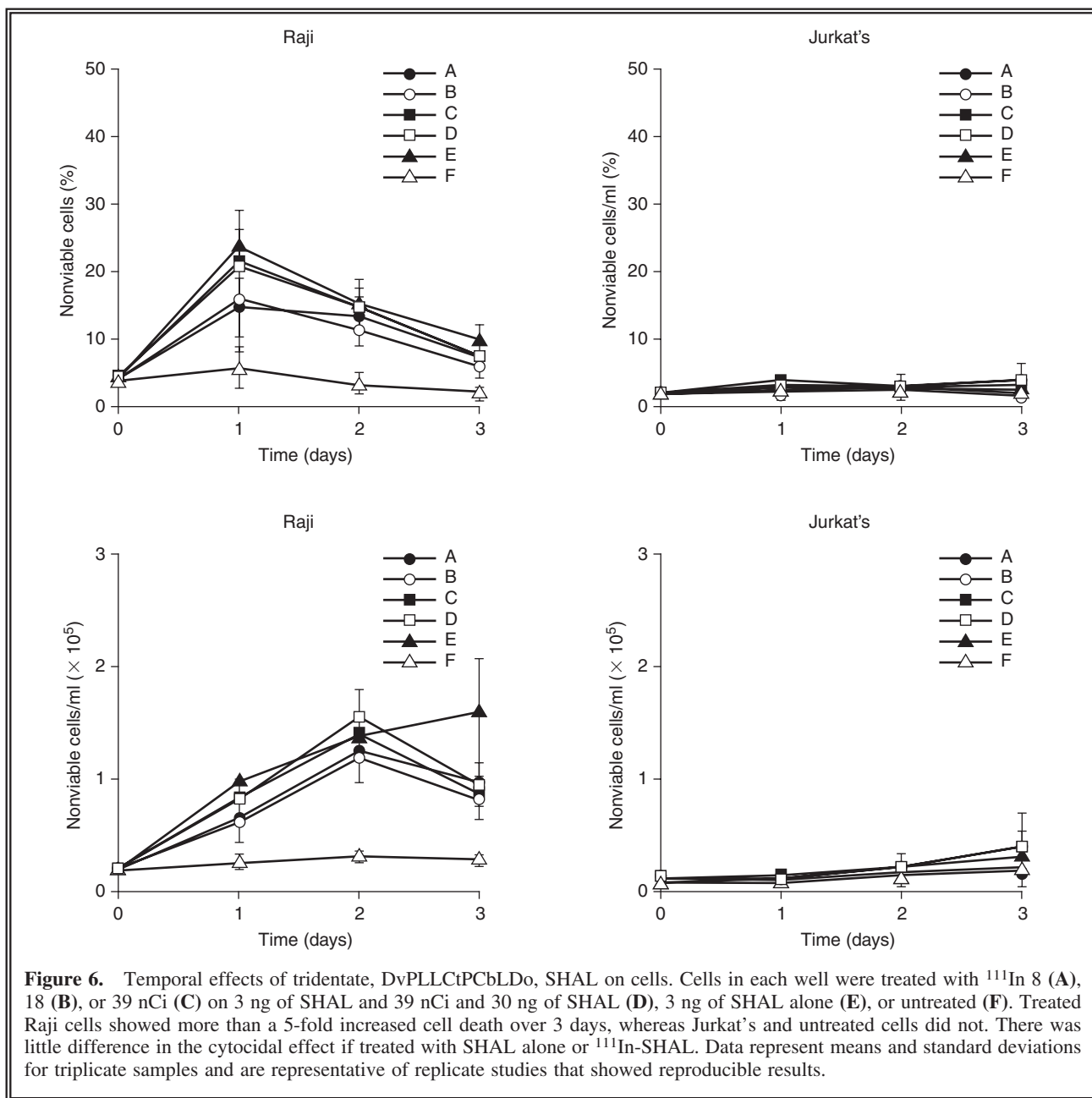


## Cell Binding, Uptake, and Residualization

The tridentate and dimeric, tridentate SHALs discriminated HLA-DR10 expressing from nonexpressing cells in enzyme-linked immunosorbent assay (ELISA) conducted at both 20° and at 4°C (Fig. 3). In assays in which incremental amounts of SHAL were added to cells, each SHAL accumulated at a fixed, fractional mass and number of moles (molecules) over a range greater than 1000 ng of added SHAL (Fig. 4). The affinities

of the SHALs could not be measured under these equilibrium conditions.

SHALs containing the Ct ligand behaved differently from the other SHALs. When compared to SHALs lacking the Ct ligand, molar uptakes of SHALs having the Ct ligand were about 3-fold greater in expressing cells before washing (Fig. 4A). After washing, residual SHAL in expressing cells was greater than 179 times more than cell-surface membrane HLA-DR10 (>412 vs. 2.3 pmoles/10<sup>6</sup> cells; >10<sup>8</sup> vs. 10<sup>6</sup> copies per Raji

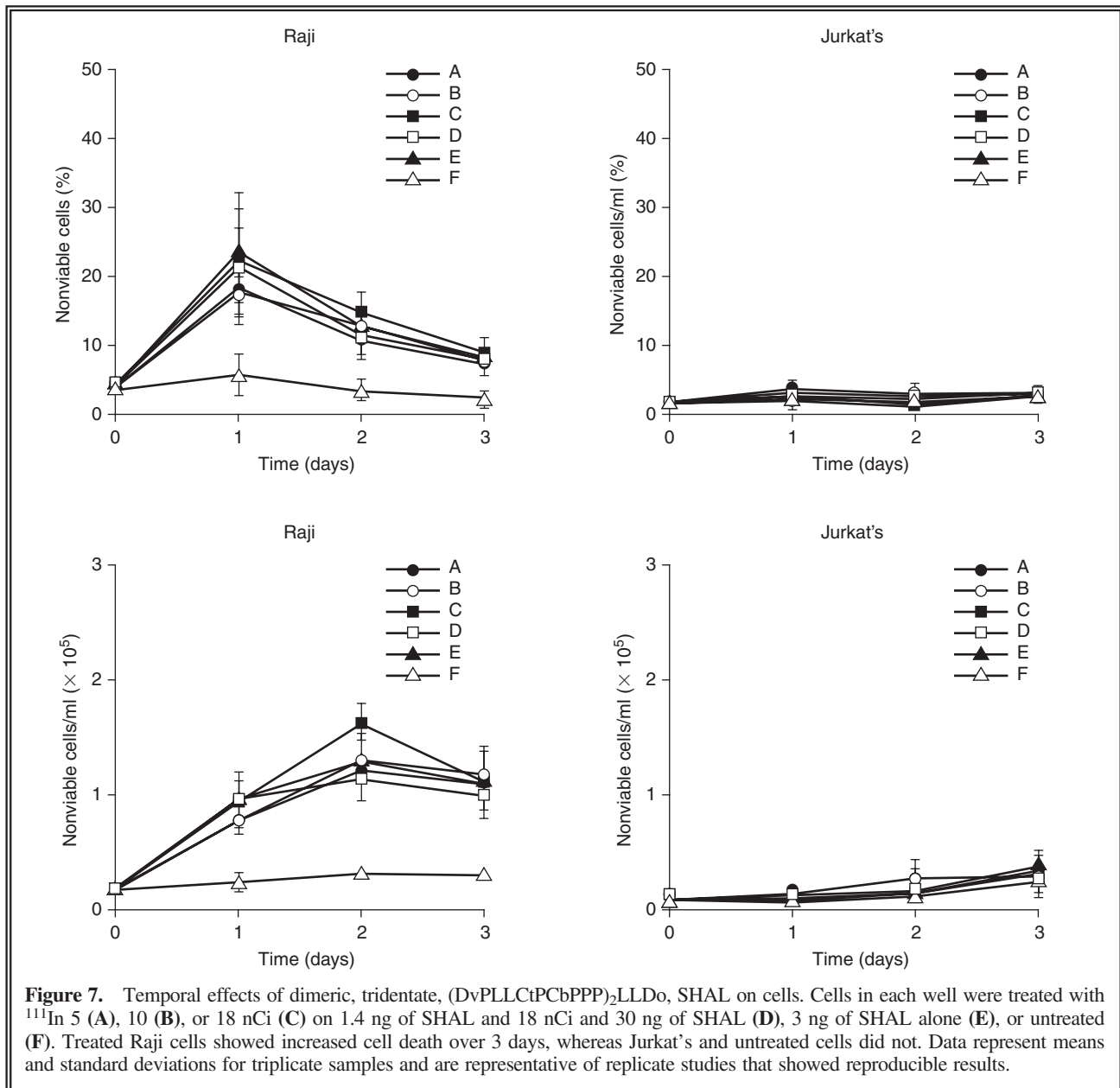


cell). Then, 3D confocal microscopy of Raji cells confirmed the intracellular location of these SHALs and the cell surface membrane location of Lym-1 (Fig. 5).

### Cytotoxicity

Both tridentate and dimeric, tridentate SHALs having the Ct ligand showed substantial anti-lymphoma (cytotoxic) effects on HLA-DR10-expressing cells at nanomolar concentrations (picomoles/mL), but not on nonexpressing cells over the 3-day interval, even in the absence of  $^{111}\text{In}$

(Figs. 6 and 7). Although the effect was not titrated, the fraction and absolute number of dead cells increased more than 5-fold, when comparing SHAL treated with untreated expressing cells or with treated or untreated nonexpressing cells. Raji, treated with tridentate or dimeric, tridentate SHALs, showed an increased number of dead cells after 2 days of exposure ( $p < 0.01$ ), whereas Jurkat's did not ( $p = 0.10\text{--}0.82$ ), when compared to untreated cells. In regression models, both the tridentate and the dimeric, tridentate SHAL significantly increased dead cells in expressing cell lines ( $p < 0.001$ ). In models with a dose-response



effect for  $^{111}\text{In}$ , but no dose-response effect for SHAL nor for  $^{111}\text{In}$  and SHAL interaction, the percent nonviable expressing cells increased linearly by about 0.5% per 5 nCi of  $^{111}\text{In}$  in the well. Based on the maximum  $^{111}\text{In}$  activity measured for the wells, the radiation-absorbed dose to the nucleus of the cells ranged from 0.11 Gy after 1 day to a maximum of 0.55 Gy after 3 days. Neither SHAL nor  $^{111}\text{In}$  had a significant effect on the nonexpressing Jurkat's or CEM cells.

## DISCUSSION

Although SHALs readily diffused into cells, they distinguished HLA-DR10 expressing from nonexpressing human, live lymphoma cells in assays.<sup>12-14</sup> Additionally, SHALs containing the Ct (3-(2-([3-chloro-5-trifluoromethyl)-2-pyridinyl]oxy)-anilino)-3-oxopropanionic acid) ligand residualized in HLA-DR10-expressing cells over a large range of added SHAL, both at RT and at 4°C, so that the HLA-DR10 copy number per expressing cell identified by the SHALs was more than 179 times the cell surface copy number identified by Lym-1 mAb. Confocal micrographs of Raji cells confirmed intracellular localization of the tridentate and dimeric, tridentate SHAL motifs, whereas Lym-1 was restricted to the cell surface (Fig. 5). Further, these SHALs had substantial cytotoxic activity on HLA-DR10-expressing Raji cells in culture, and also in xenografts in mice (preliminary data, not shown), such as that of Lym-1 and at SHAL concentrations readily achievable in patients. SHALs lacking the Ct ligand, SHAL diluents, and nonspecific mAbs have not shown cytotoxic effects, whereas Lym-1 has shown greater cytotoxic apoptotic effects in cell culture and in xenografts in mice than rituximab.<sup>5,6,12</sup> The anti-lymphoma effects of the SHALs on Raji cells and xenografts were similar to those of Lym-1 and greater than those of rituximab.

As part of the immune mechanism, histocompatibility proteins bind peptides and present them on the surface of expressing cells.<sup>23</sup> These proteins are also important receptors that have been shown to participate in transmembrane and cytoplasmic signaling.<sup>24-26</sup> Although upregulated on the surface membrane of human malignant B-cells, HLA proteins are even more abundant inside these cells (Fig. 8), where they are manufactured and assembled on the endoplasmic reticulum. Some cell-surface proteins internalize by their nature or after ligation.<sup>27</sup> HLA-DR-receptor proteins internalize and the

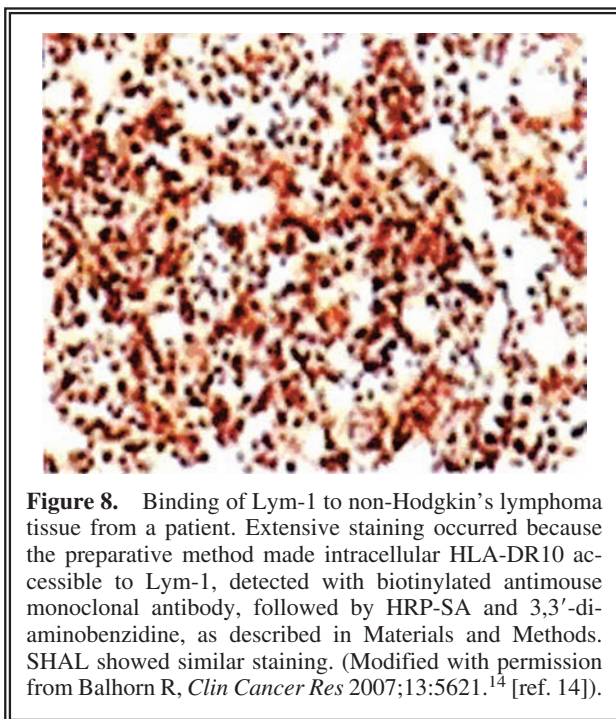


**Figure 8.** Binding of Lym-1 to non-Hodgkin's lymphoma tissue from a patient. Extensive staining occurred because the preparative method made intracellular HLA-DR10 accessible to Lym-1, detected with biotinylated antimouse monoclonal antibody, followed by HRP-SA and 3,3'-diaminobenzidine, as described in Materials and Methods. SHAL showed similar staining. (Modified with permission from Balhorn R, *Clin Cancer Res* 2007;13:5621.<sup>14</sup> [ref. 14]).

SHALs containing the Ct ligand internalized and residualized, functioning like a "Trojan horse," in HLA-DR10-expressing cells. This likely accounts for our observation that SHALs containing the Ct ligand identified more than 179 times the number of HLA-DR-binding sites (copies) than Lym-1 identified cell-surface HLA-DR protein on Raji cells. Additionally, internalized SHALs were positioned to deposit radiation and other toxins near the DNA, where their effects are more potent and selective.

Lym-1 mAb is a useful radionuclide carrier for therapy and imaging and binds with lymphoma tissue from about 90% of patients with B-cell NHL.<sup>16,28</sup> Although not modulated when ligated to HLA-DR protein,<sup>16</sup> some Lym-1 internalization in malignant B-lymphocytes has been reported.<sup>29</sup> Most mAbs, but not Lym-1, when internalized, are promptly catabolized and released.<sup>29</sup>

Our SHALs bind within the Lym-1 epitopic region of HLA-DR protein, have a molecular weight less than 5 kDa, and are rapidly excreted.<sup>11,14</sup> To further increase cell selectivity and binding, tridentate SHALs, having a third ligand, and dimeric SHALs, emulating multivalent mAb binding, have been generated. SHALs have been readily produced, which included a chelator to which metals and lanthanides can be attached for magnetic resonance and nuclear imaging and for

radiotherapy. Additionally, the lysine residues in the linkers can also be used to attach other radionuclides and functionalities.<sup>30</sup> All of these mAb mimetics have exhibited selectivity for the target protein, have been labeled with radionuclides in high yield and purity, and are expected to have a long shelf-life and potential for oral administration. Gram amounts can be synthesized for a fraction of the cost of biologicals.

The Ct ligand imparted several important properties on the SHALs. The mechanisms underlying these properties are of interest. Differences in the cellular behavior of SHALs having, and lacking, the Ct ligand were not accounted for by differences in SHAL size or dimerism. Presently, we interpret the observations as follows. After binding to HLA-DR10 proteins on the surface membrane of expressing cells, the protein and associated SHAL were endocytosed and carried to sites where the SHAL was unavailable for exchange with media outside the cell. Possible explanations for the special characteristics of Ct ligand SHALs include: 1) the Ct ligand in the SHAL bound to a site on HLA-DR10 protein that increased cell signaling; 2) the Ct ligand improved SHAL ability to penetrate the cell-surface membrane after HLA-DR10 binding; 3) the Ct ligand improved binding to HLA-DR10 on the cell surface and/or inside the cell; and 4) the Ct ligand exhibited pH effects when intracellular. The properties exhibited by SHALs containing the Ct ligand and their mechanisms are deserving of further study, including the ligand's cytotoxic effects and potential for transporting agents to critical cell locations. Ct analogs have been shown by others to inhibit fatty-acid synthesis via acetylCoA carboxylase,<sup>31</sup> and to have antifungal<sup>32</sup> and herbicidal activity.<sup>33</sup> This is a fertile area for additional investigation, particularly because other small molecules have been shown to have antagonist or agonist functions useful for treating cancer.<sup>34</sup>

Irradiating DNA is also an effective way to kill cells. The use of mAbs as radionuclide carriers has improved response rates and patient acceptance, when compared to immunotherapy and chemotherapy, respectively.<sup>1,3</sup> Lym-1-induced cell death is increased by the addition of a radionuclide.<sup>4</sup> Further, a radionuclide localized inside the cell has improved efficacy and specificity, if its emission ranges are short; Auger electrons inside the cell are efficient for inducing lethal effects.<sup>30</sup> If radionuclides that emit both photon and Auger radiations are used, both imaging and radiotherapy can be achieved. The <sup>111</sup>In, used in this study, is such a radionuclide and, like

the Ct containing SHALs, is also capable of residualizing inside the cell.<sup>35</sup>

## CONCLUSIONS

SHALs containing the Ct ligand selectively bound to, residualized inside, and were cytotoxic for HLA-DR10-expressing human lymphoma cells. The ability of these SHALs to directly and selectively induce cell death suggests that SHAL binding to HLA-DR10 triggered cell signaling. The tridentate and dimeric, tridentate SHALs described in this paper provide extraordinary opportunities for molecular therapy and imaging. The technology established to target HLA-DR10, and related HLA-DRs, can be modified to transport and residualize toxic agents near critical sites inside other malignant cells, using other proteins as targets.

## ACKNOWLEDGMENTS

This work was supported by National Cancer Institute PO1-CA47829 and Lawrence Livermore National Laboratory Awards 01-ERD-111, 01-ERD-046, and 01-SI-012. The authors thank B. Pettit for manuscript preparation.

## DISCLOSURE STATEMENT

No competing financial interests exist.

## REFERENCES

1. Witzig TE, Gordon LI, Cabanillas F, et al. Randomized, controlled trial of yttrium-90-labeled ibritumomab tiuxetan radioimmunotherapy versus rituximab immunotherapy for patients with relapsed refractory low-grade, follicular, or transformed B-cell non-Hodgkin's lymphoma. *J Clin Oncol* 2002;20:2453.
2. Kaminski MS, Zelenetz AD, Press OW, et al. Pivotal study of iodine I <sup>131</sup>tositumomab for chemotherapy-refractory low-grade or transformed low-grade B-cell non-Hodgkin's lymphomas. *J Clin Oncol* 2001;19:3918.
3. DeNardo GL, Sysko VV, DeNardo SJ. Cure of incurable lymphoma. *Int J Radiat Oncol Biol Phys* 2006; 66(Suppl 2):s46.
4. DeNardo GL, Tobin E, Chan K, et al. Direct antilymphoma effects on human lymphoma cells of monotherapy and combination therapy with CD20 and HLA-DR

- antibodies and yttrium-90 HLA-DR antibodies. *Clin Cancer Res* 2005;11:7075.
5. Tobin E, DeNardo GL, Zhang N, et al. Combination immunotherapy with anti-CD20 and anti-HLA-DR monoclonal antibodies induces synergistic antilymphoma effects in human lymphoma cell lines. *Leuk Lymph* 2007; 48:944.
  6. Zhang N, Khawli LA, Hu P, et al. Lym-1-induced apoptosis of non-Hodgkin's lymphomas produces regression of transplanted tumors. *Cancer Biother Radiopharm* 2007;22:342.
  7. Rose LM, Gunasekera AH, DeNardo SJ, et al. Lymphoma-selective antibody Lym-1 recognizes a discontinuous epitope on the light chain of HLA-DR10. *Cancer Immunol Immunother* 1996;43:26.
  8. Rose LM, Deng CT, Scott S. Critical Lym-1 binding residues on polymorphic HLA-DR molecules. *Mol Immunol* 1999;36:789.
  9. Kramer RH, Karpen JW. Spanning binding sites on allosteric proteins with polymer-linked ligand dimers. *Nature* 1998;395:710.
  10. Hajduk PJ, Meadows RP, Fesik SW. Discovering high-affinity ligands for proteins. *Science* 1997;278:497.
  11. DeNardo GL, Natarajan A, Hok S, et al. Pharmacokinetic characterization in xenografted mice of a series of first generation mimics for HLA-DR antibody, Lym-1, as carrier molecules to image and treat lymphoma. *J Nucl Med* 2007;48:1338.
  12. West J, Perkins J, Hok S, et al. Direct antilymphoma activity of novel, first-generation "antibody mimics" that bind HLA-DR10-positive non-Hodgkin's lymphoma cells. *Cancer Biother Radiopharm* 2006;21: 645.
  13. Balhorn R, Hok S, Burke P, et al. Selective high-affinity ligand antibody mimics for cancer diagnosis and therapy: Initial application to lymphoma/leukemia. *Clin Cancer Res* 2007;13(Suppl 18):5621s.
  14. DeNardo GL, Hok S, Natarajan A, et al. Characteristics of dimeric (bis) bidentate selective high-affinity ligands as HLA-DR10 beta antibody mimics targeting non-Hodgkin's lymphoma. *Int J Oncol* 2007;31:729.
  15. Hok S, Natarajan A, Balhorn R, et al. Synthesis and radiolabeling of selective high-affinity ligands designed to target non-Hodgkin's lymphoma and leukemia. *Bioconjug Chem* 2007;18:912.
  16. Epstein AL, Marder RJ, Winter JN, et al. Two new monoclonal antibodies, Lym-1 and Lym-2, reactive with human-B-lymphocytes and derived tumors, with immunodiagnostic and immunotherapeutic potential. *Cancer Res* 1987;47:830.
  17. Kuntz ID, Blaney JM, Oatley SJ, et al. A geometric approach to macromolecule-ligand interactions. *J Mol Biol* 1982;161:269.
  18. Desjarlais RL, Sheridan RP, Seibel GL, et al. Using shape complementarity as an initial screen in designing ligands for a receptor binding site of known three-dimensional structure. *J Med Chem* 1988;31:722.
  19. Albrecht H, Cosman M, Ngu-Schwemlein M, et al. Recombinant expression of the b subunit of HLA-DR10 in the selection of novel lymphoma targeting molecules. *Cancer Biother Radiopharm* 2007;22:531.
  20. Scatchard G. The attraction of proteins for small molecules and ions. *Ann N Y Acad Sci* 1947;51:660.
  21. Goddu SM, Howell RW, Rao DV. Cellular dosimetry: Absorbed fractions for monoenergetic electron and alpha particle sources and S-values for radionuclides uniformly distributed in different cell compartment. *J Nucl Med* 1994;35:303.
  22. Ong GL, Elsamra SE, Goldenberg DM, et al. Single-cell cytotoxicity with radiolabeled antibodies. *Clin Cancer Res* 2001;7:192.
  23. Watts C. Capture and processing of exogenous antigens for presentation on MHC molecules. *Ann Rev Immunol* 1997;15:821.
  24. Leveille C, Cataigne JG, Charron D, et al. MHC class II isotype-specific signaling complex on human B-cells. *Eur J Immunol* 2002;32:2282.
  25. Klemm JD, Schreiber SL, Crabtree GR. Dimerization as a regulatory mechanism in signal transduction. *Annu Rev Immunol* 1998;16:569.
  26. Lane PJ, McConnell FM, Schieven GL, et al. The role of class II molecules in human B-cell activation. *J Immunol* 1990;144:3684.
  27. Cescato R, Schulz S, Waser B, et al. Internalization of sst2, sst3, and sst5 receptors: Effects of somatostatin agonists and antagonists. *J Nucl Med* 2006;47:502.
  28. DeNardo GL, DeNardo SJ, Goldstein DS, et al. Maximum tolerated dose, toxicity, and efficacy of <sup>131</sup>I-Lym-1 antibody for fractionated radioimmunotherapy of non-Hodgkin's lymphoma. *J Clin Oncol* 1998;16:3246.
  29. Ong GL, Mattes MJ. Processing of antibodies to the MHC class II antigen by B-cell lymphomas: Release of Fab-like fragments into the medium. *Mol Immunol* 1999;36:777.
  30. Costantini DL, Chan C, Cai Z, et al. <sup>111</sup>In-labeled trastuzumab (herceptin) modified with nuclear localization sequences (NLS): An Auguer electron-emitting radiotherapeutic agent for HER2/neu-amplified breast cancer. *J Nucl Med* 2007;48:1357.
  31. Zhang H, Tweel B, Tong L. Molecular basis for the inhibition of the carboxyltransferase domain of acetyl-coenzyme-A carboxylase by haloxyfop and diclofop. *Proc Natl Acad Sci U S A* 2004;101:5910.
  32. Yu C-R, Xu L-H, Tu S, et al. Synthesis and bioactivity of novel (3-chloro-5-(trifluoromethyl)pyridin-2-yloxy) phenyl containing acrylate and acrylonitrile derivatives. *J Fluorine Chem* 2006;127:1540.
  33. Zagnitko O, Jelenska J, Tevzadze G, et al. An isoleucine/leucine residue in the carboxyltransferase domain of acetyl-CoA carboxylase is critical for interaction with aryloxyphenoxypionate and cyclohexanedione inhibitors. *Proc Natl Acad Sci U S A* 2001;98:6617.
  34. Arkin MR, Wells JA. Small-molecule inhibitors of protein-protein interactions: Progressing towards the dream. *Nat Rev Cancer* 2004;3:301.
  35. Press OW, Howell-Clark J, Anderson S, et al. Retention of B-cell-specific monoclonal antibodies by human lymphoma cells. *Blood* 1994;83:1390.

